scientific reports

Check for updates

OPEN

Preparation and characterization of biodegradable cellulose nanofiber films modified with methylene blue and vitamin C for detecting oxidants

Sina Sadeghi[1], Sajad Pirsa[2]✉, Narmela Asefi[1] & Mehdi Gharekhani[1]

In this study, cellulose nanofiber film was modified with methylene blue (MB) dye and vitamin C (Cel/MB/VC). The physicochemical and antibacterial characteristics of the prepared films were investigated. The rate of absorption and release of MB from the prepared film was studied. Films containing MB and VC were used as a kit to detect hydrogen peroxide. The results showed that MB and VC increased the thickness of the film and the elongation of the film. Both MB and VC agents reduced moisture and water vapor permeability, which significantly increased the antioxidant and antimicrobial properties (against *Escherichia coli* and *Staphylococcus aureus*) of the film. SEM images showed that the diameter of cellulose fibers is between 20 and 100 nm, which MB and VC completely cover their surface and the surface porosity of the film. FTIR spectra confirmed the electrostatic interactions between cellulose, MB and VC. According to the XRD results, cellulose has a crystalline structure, which is improved further on the vitamin C is added. According to TGA, MB and VC promoted thermal stability of the cellulose films. The release of methylene blue from the film was reported to be 15%. In the presence of H_2O_2, the color of the films containing MB and VC changed from white to blue, and that showed good performance as a hydrogen peroxide detection sensor (kit). The highest sensitivity of the sensor for measuring H_2O_2 was 0.299 (100 mg/ml) with a detection limit of 1.9 (100 mg/ml).

Keywords Biodegradable film, Kit, Oxidation/regeneration, Antioxidant, Antibacterial

The release of petroleum polymers into the environment causes environmental pollution and creates many biological problems for humans and animals[1]. Due to the fact that these polymers are not easily decomposed, the use of these polymers in various industries, including food packaging, faces many problems[2]. Therefore, in recent years, the use of biodegradable polymers in food packaging has become very popular. Biodegradable polymers of plant and biological origin can be a good substitute for petroleum polymers. While these polymers have suitable chemical properties like these polymers are easily broken down by bacteria, they are easily decomposed when released in the environment and do not have environmental pollution problems[3–5]. Biopolymers with protein, polysaccharide and lipid structures or their composites are used to produce biodegradable plastics[6]. Cellulose and its derivatives are of special importance among different biological sources for the preparation of biodegradable films. Most of cellulose derivatives are biodegradable and renewable resources[7]. Cellulose-derived compounds are usually considered non-toxic and non-allergenic. Derivatives include cellulose nanofiber, celluloid, cellulose acetate, methylcellulose, hydroxypropylmethylcellulose and carboxymethylcellulose, all of which are used in the preparation of biodegradable films. Because cellulose is found in nature easily and is relatively cheap, and its structure can be modified easily[8–11]. It is a complex carbohydrate or polysaccharide consisting of hundreds to thousands of glucose molecules linked together forming chains. Unlike animals, plants (like cotton), algae (like *Spirulina platensis*) and some bacteria (like *Acetobacter xylinus*) have the ability to produce this substance[12,13].

MB is a crystalline substance and a type of organic chloride salt that is classified as a thiazine dye. Methylene blue initially has a powdery texture and is very dark green, but when dissolved in water, its color changes to dark blue[14]. The reason for this color change can be said to be that methylene blue, when dissolved in water,

[1]Department of Food Science and Technology, Tabriz Branch, Islamic Azad University, Tabriz, Iran. [2]Department of Food Science and Technology, Faculty of Agriculture, Urmia University, Urmia, Iran. ✉email: Pirsa7@gmail.com; S.pirsa@urmia.ac.ir

will be affected by oxidizing agents and for this reason, it loses its electrons. On the other hand, the ionic bonds of methylene blue are transformed into ionic components when placed in water. This substance works well as an indicator; It will detect the amount of oxygen present in various solutions[15]. MB is a functional dye that acts as a redox indicator and has different colors (blue/colorless) in oxidized or reduced states. One of the tests to determine the quality of milk, with which the number of bacteria in raw milk is estimated, is the MB regeneration test[16]. The degradation mechanisms of MB mainly involve photochemical and chemical processes. One of the key methods is photocatalytic degradation, in which semiconductor nanomaterials under UV or visible light irradiation produce reactive species that can degrade MB[17].

Vitamin C is an antioxidant (or regenerative agent) that has the ability to prevent damage from free radicals and dangerous chemicals. Free radicals play a role in the occurrence of some diseases, including cancer, heart disease and arthritis. The use of vitamin C in the structure of biodegradable polymers can make these polymers an active antioxidant composite. Therefore, the use of biodegradable polymers containing vitamin C can be used in food packaging and increase the shelf life of foods sensitive to oxidation[18,19].

Active and smart packaging are among the new packaging methods that have attracted the attention of many scientists[20,21]. Kits (color sensors) sensitive to the concentration of carbon dioxide, labels sensitive to the amount of oxygen, time-temperature labels and labels sensitive to changes in the pH of food are among the kits that are recently used in the smart packaging of food products[22]. Packages containing smart kits, due to having special identifiers, can detect environmental conditions and changes in food and provide consumers with information about the quality and whether the food is healthy or unhealthy by means of these indicators. Smart food packaging does not work directly to increase the shelf life of food, but rather provides information about food quality to stakeholders in food supply chains[23].

In this research, an active and intelligent biodegradable film was designed that, in addition to being able to slow down the oxidation of food and increase its shelf life, at the same time, it can intelligently monitor the oxidation process in food products and increase its shelf life and estimate its expiration date. For this purpose, cellulose nanofiber film modified with MB and VC was used to prepare smart film. Methylene blue has a blue color in its natural state, which becomes colorless in the composite with VC (as a reducing agent). Therefore, cellulose film modified with MB and VC is a white film. This film has the ability to detect the oxidizing agent. In this research, hydrogen peroxide was used as a soft oxidant to investigate the sensing behavior of the prepared cellulose film. Using mathematical equations, linear relationships were established between the color changes of the sensor and the concentration of hydrogen peroxide, and it was used for qualitative and quantitative measurement of hydrogen peroxide. The obtained results showed that the cellulose film modified with MB and VC has suitable physicochemical properties to be used as a smart marker in food packaging and can identify and measure hydrogen peroxide as a smart marker.

Materials and methods

Chemicals

Cellulose film with Nano fibrous structure (thickness 30 to 100 nm) and porosity 5 to 10 micrometers (molecular weight 100,000 to 200,000 Daltons) was obtained from Zardab Tabriz (Iran). Hydrogen peroxide (35%), MB (99% purity), VC (99% purity), sodium hydroxide, silica gel, and other chemical compounds used were obtained from Merck (Germany) and Aldrich (USA) companies and were used without further purification. All used chemicals have a purity of more than 98%.

Preparation of cel/mb/vc film

To prepare standard MB solution, 500 mg of commercial MB powder was dissolved in 1 L of distilled water. Dissolution was continued at room temperature while stirring for 10 min. In order to prepare films, first, cellulose films were prepared in dimensions of 10 × 10 cm (1 g). In a 100 ml beaker, 50 ml of distilled water was added and some MB solution was added to it at three levels (0, 50 and 100 µL - according to the Table 1) and

Film	A: Methylene blue (µL)	B: Vitamin C (%)
1	50	5.0
2	50	0.0
3	100	0.0
4	50	2.5
5	0	0.0
6	50	2.5
7	100	5.0
8	0	2.5
9	50	2.5
10	0	5.0
11	100	2.5
12	50	2.5
13	50	2.5

Table 1. List of films prepared based on the CCD.

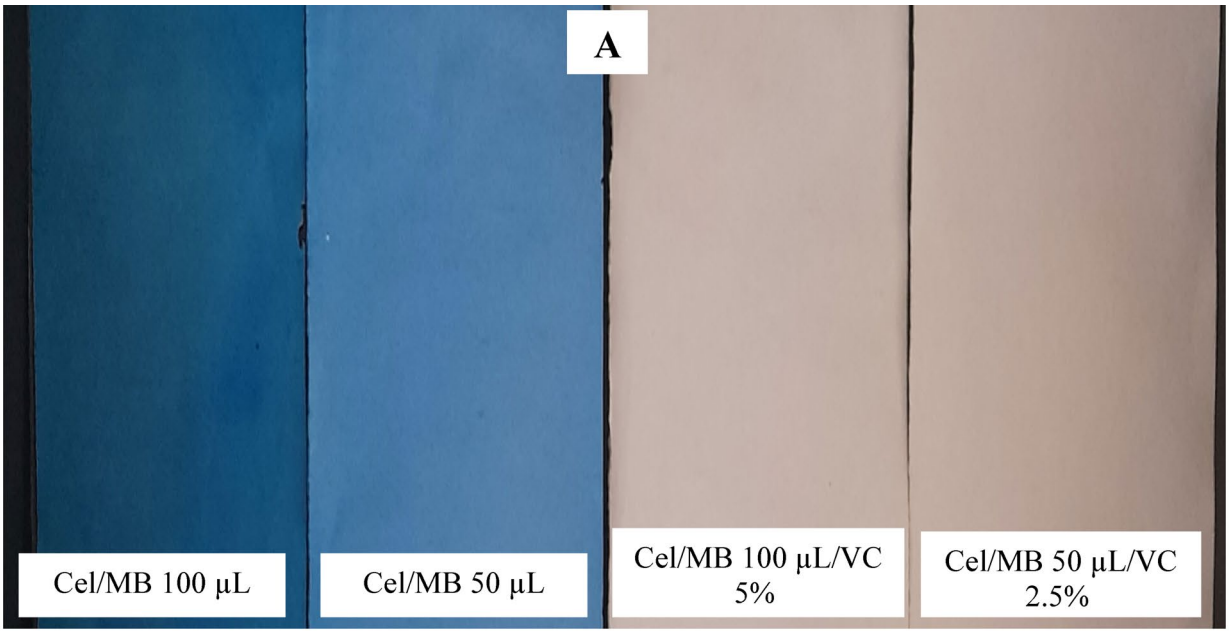

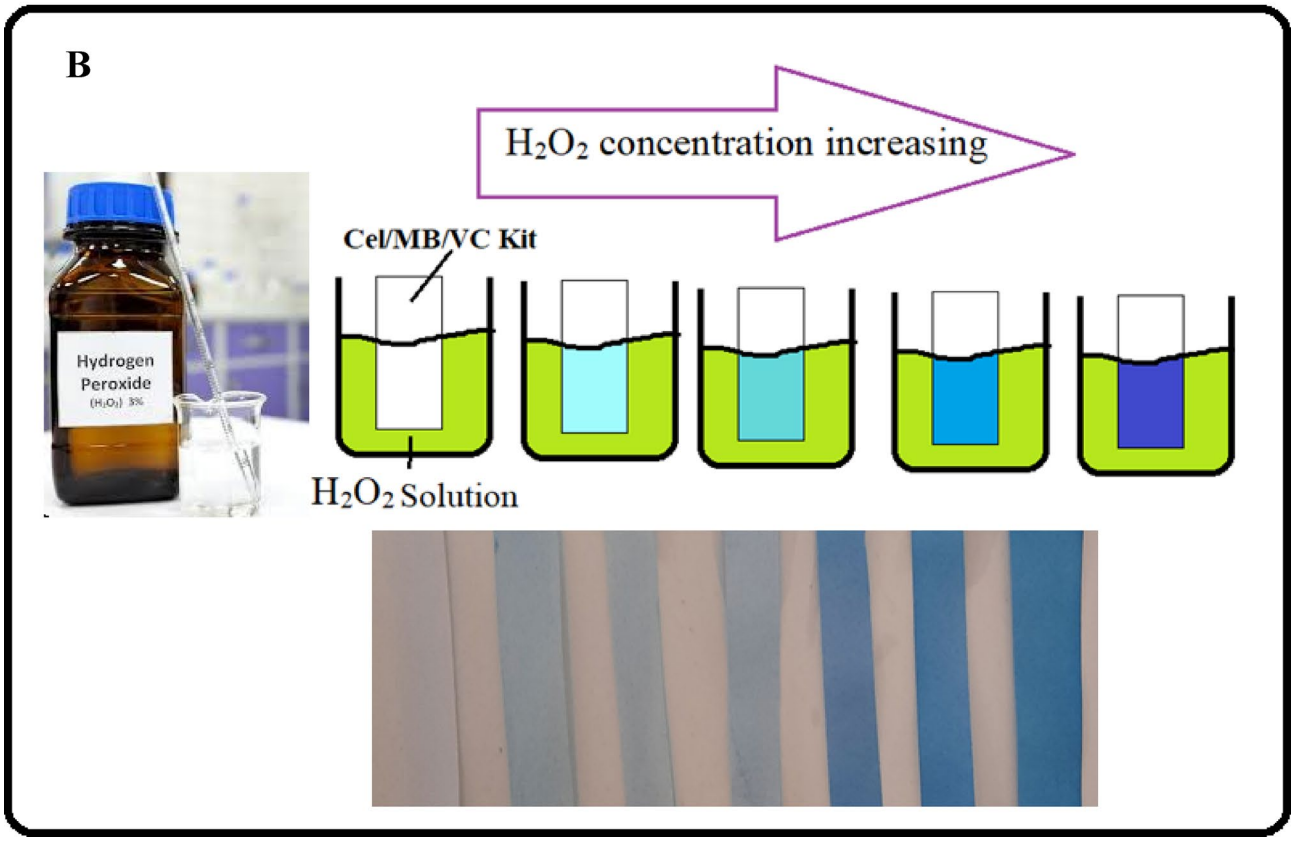

Fig. 1. Cellulose films modified with MB and VC (**A**), the effect of H_2O_2 on the color changes of Cel/MB/VC film (**B**) and the system for measuring color characteristics (**C**).

dissolved. Next, the cellulose film was immersed in the prepared solution for 10 min. After 10 min, the blue film was removed from the solution and dried in an oven at 50 °C. Then the colored film was immersed in 50 ml of 5% NaOH solution for 10 min. Then the film was removed from the solution and dried again in the oven at 50 °C. The dried film was immersed in a solution containing VC at three levels (0, 2.5 and 5% - according to the Table 1) for 10 min. At this stage, the color of the film turned white. At the end, the film was removed from the solution and dried in an oven at 50 °C (Fig. 1-A). The dried films were stored in black plastic bags at refrigerator temperature until the tests were performed.

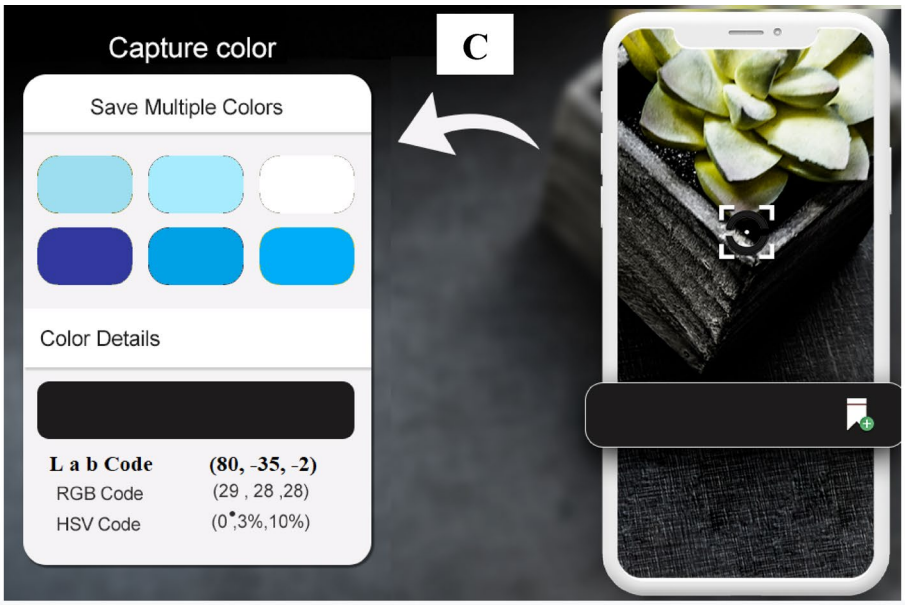

Fig. 1. (continued)

Physical and chemical characteristics of the prepared films

Thickness

The thickness of each film was measured at 5 different points. The obtained numbers were averaged and reported. The thickness of the film was used to determine mechanical resistance and water resistance, etc. In this test, a digital micrometer (Insize Digital Outside Micrometer 3108–25 A) was used.

Mechanical characteristics

The mechanical properties of the films include elongation at breaking point (EAB) and tensile strength (TS) are important factors for food packaging. To check the mechanical properties, the samples were conditioned for 24 h in special conditions. Special conditions included relative humidity RH = 55%. The films were cut with a special cutter in dimensions of 1 × 8 cm in a dumbbell shape. The films were placed between the two jaws of the device, and the initial distance between the two jaws is 50 mm. The upper jaw was moved relative to the lower jaw at a speed of 5 mm/min. The mechanical properties were recorded by a computer. A Texture analyzer-brand histometer (Zwick/Roell model FR010, Germany) was used to perform this test.

Moisture content

To measure the moisture of the films, first the films was cut into 3 × 3 cm dimensions. Then, the cut films were kept in a desiccator for 24 h in specific humidity conditions (55% relative humidity) at a temperature of 25 °C. The desiccator contained silica gel. At this stage, the weight of the films was measured and recorded as the initial weight. Then, in order to completely remove the moisture from the films, the film sample was heated at 100 °C for 2 h and finally its final weight was measured and recorded. The following equation was used to calculate the moisture content of the film.

$$\text{Humidity}(\%) = \frac{\boldsymbol{W_i} - \boldsymbol{W_f}}{\boldsymbol{W_i}} \times 100 \quad (1)$$

Wi: Initial film weightWf: Final film weight

Water vapor permeability

Permeability relative to water vapor was measured by gravimetric method. For this test, the test film was sealed in a glass vial with a height of 4 cm containing silica gel to maintain 0% relative humidity (RH 0%) in the vial. The vials had an inner diameter of 6.4 cm and their outer diameter was 8.9 cm. Also, the exposed surface of the vials was 26 cm^2. The vials were placed in a controlled temperature (38 ± 1 °C) and relative humidity (90 ± 3%). The transfer of water vapor was determined from the increase in the weight of the vial. Changes in cell weight were recorded as a function of time. The slope of weight changes versus time (after reaching steady state) was

calculated by linear regression. Water vapor transmission rate (WVTR) was defined as the slope (g/d) divided by the transfer area (m^2). After penetration tests, WVP was calculated as follows[24]:

$$WVP = \frac{WVTR \times X}{\Delta p} \ [g, \mu/m^2/d/kPa] \quad (2)$$

Where X is the thickness of the paper and Δp is the partial pressure difference of water vapor throughout the film and its numerical value is 9.5 kPa.

Antioxidant property
DPPH (2,2-diphenyl-1-picrylhydrazy) radical quenching method was used to measure the antioxidant power of the films. For this test, to prepare film extract, 25 mg of each film was dissolved in 4 ml of distilled water for 2 min. Then, 2.8 ml of film extract solution was mixed with 1 mM methanolic DPPH solution (0.2 ml). The obtained solution was stirred with a vortex 2000 rpm for 2 min and kept in a dark place for 1 h. The absorbance of the solution was recorded using a spectrophotometer (Model T60 UV, USA) at a wavelength of 517 nm. The following equation was used to calculate the antioxidant percentage.

$$\text{Antioxidant activity}(\%) = \frac{A_b - A_s}{A_b} \quad (3)$$

A_b: Absorption rate of the control sample (DPPH methanolic solutions: 1 mM)A_s: Sample absorption rate

Antibacterial activity
Agar diffusion method was used to determine the antibacterial property of the films. For this purpose, the films were cut into discs (with a diameter of 15 mm) and then placed on Mueller Hinton agar plates containing *Staphylococcus aureus* ATCC6538 and *Escherichia Coli* ATCC13706, with a concentration of (10^7 CFU/mL). took The plates were incubated for 24 h at 37 °C. After 24 h, the radius of bacterial non-growth halos around the films (in millimeters) was measured with a precision caliper.

Scanning electron microscopy
The technique of scanning electron microscope (SEM) (ZEISS, SIGMA, Germany) was used to investigate the polymer structure, surface characteristics, porosity and particle distribution of the prepared films. In this method, the surface of the film samples was covered with a thin layer of gold before analysis. The accelerator voltage of 20 kV was used for the adjustment device. The prepared samples were placed in a special position of the device and photographs were taken of the sample surface at different magnifications.

Fourier transform infrared spectroscopy
Fourier Transform Infrared (FTIR) device (Tensor 27, Bruker, Germany) was used to investigate physical or chemical interactions between film components. To perform this test, first the films was dried and completely powdered. The obtained powder was mixed with KBr at a ratio of 1 to 20. The powder mixture was turned into a thin film with a special pressing machine. FTIR spectra of each sample were recorded separately. The spectrum of the samples was recorded with a resolution of 4 cm^{-1} and number of scans (16) in the range of 400–4000 cm^{-1}.

X-ray diffraction
X-ray diffraction (XRD) technique was used with the help of X-ray diffractometer (Kristalloflex D500, Siemens, Germany) to check the crystalline or amorphous structure. In this technique, first, the film samples were placed in the special position of the device (sample cell). The primary rays were irradiated to the sample at ambient temperature and the reflected rays were collected in the range of angle 2θ = 0–80° at a rate of 2 degrees/min. The XRD spectra of the samples were drawn automatically by the machine. Cu Kα radiation source was used at a wavelength of 0.154 nm. The specifications of the device include X-ray generator at 40 kV and 40 mA.

Thermogravimetric analysis
To check the thermal stability of the films, the Thermogravimetric analysis (TGA) test was used by a thermal analyzer (Linseis – L81A1750, Germany). For this purpose, films were prepared in the form of 10 mg samples. The film samples were heated under a nitrogen atmosphere of 50 cm^3/min in aluminum cups in the temperature range of 30–600 °C. The heating rate was 10 °C/min. The empty aluminum cup was considered as a reference and the TGA curve was drawn and recorded by the device.

Absorption and release of MB

To check the absorption of MB, the UV-Vis spectrum of the solutions used to prepare the film was measured before and after the absorption of MB by the film, and the amount of absorption was calculated from the decrease in the intensity of the absorption peak at the wavelength of 665 nm (Eq. 4). To check the release rate, the films containing MB were immersed in 100 ml of distilled water and after 24 h, the absorbance of the solution was measured at the wavelength of 665, and the release rate of MB was checked from Eq. 5.

$$Absorption\ (\%) = \frac{A_{MB1} - A_{MB2}}{A_{MB1}} \times 100 \quad (4)$$

Film	A: Methylene blue (µL)	B: Vitamin C (%)
Control (Pure Cellulose)	0	0
Cel/MB	100	0
Cel/VC	0	5
Cel/MB/VC	100	5

Table 2. List of films prepared for antimicrobial and antioxidant properties.

Kit	A: Methylene blue (µL)	B: Vitamin C (%)
K1	50	2.5
K2	50	5
K3	100	2.5
K4	100	5

Table 3. List of films used as oxidizing agent identification kit.

$$Release\ (\%) = \frac{A_{\mathrm{MBi}} - A_{\mathrm{MBr}}}{A_{\mathrm{MBi}}} \times 100 \tag{5}$$

In this regard, A_{MB1} is the absorption rate of MB solution before coating on cellulose film and A_{MB2} is the absorption rate of MB solution after coating on cellulose film. Also, A_{MBi} is the absorption of the initial solution (standard) of MB, and A_{MBr} is the absorption of the released solution of MB.

Cel/MB/VC film sensing behavior

Color characteristics of the sensor

In this step, the color factors of the used films were analyzed. Considering that the film changed from white to blue, factor b was further investigated. In this factor, negative numbers indicate the intensity of the blue color, and as the number moves towards more positive numbers, the blue color decreases. To record color features, the system designed in previous studies was used (Fig. 1-C)[25].

Calibrating the sensor and sensing H_2O_2

Hydrogen peroxide was used as a soft oxidant to calibrate the sensor and check the response of the sensor to oxidizing agents. Based on this, different concentrations of hydrogen peroxide were prepared and placed in contact with the sensor, and the response of the sensor was calculated with the Eq. 6. Finally, the calibration curve of the sensor was drawn as the response of the sensor to different concentrations of hydrogen peroxide and the figures of merit of the sensor were calculated.

$$Response = \frac{b_1 - b_0}{b_0} \times\ 100 \tag{6}$$

In this regard, b_0 is the value of b factor before contact with hydrogen peroxide and b_1 is the value of b factor after contact with hydrogen peroxide.

Statistical analysis

The statistical analysis and analysis of the data obtained in this research was done in three parts. In order to examine the effect of two factors, the amount of MB and VC on the physicochemical properties of the film (thickness, mechanical properties, moisture, solubility, WVP and antioxidant property), the central composite design (CCD) was used (Table 1). Design Expert-10 software was used to design experiments and analyze data at the 95% probability level and analyze variance and compare averages. In the second part, a factorial design was used at the 95% probability level to investigate the effect of two factors, the amount of MB and VC on antimicrobial properties, surface morphology, etc. (Table 2). To check the capability of the prepared films in identifying oxidizing agents (hydrogen peroxide), films containing MB and VC were used (Table 3).

Results and discussion

In this study, the response surface method was used to investigate the effect of independent variables (MB amount and VC amount) on dependent variables (thickness, mechanical properties, moisture and WVP). Table 4 shows mathematical models obtained from response surface method. In this table, the regression coefficients and adjusted regression coefficients of the obtained mathematical models are also displayed. The probability level of 95% has been used for modeling and checking the effect coefficients of different variables.

Response	Equations	R^2	R^2_{Adj}
Thickness (mm)	=+112.46 + 9.67*A + 7.83*B	0.79	0.75
TS (MPa)	=+17.07–3.17*A-2.17*B + 1.00*A*B-0.74*A2 + 2.26*B2	0.89	0.82
EAB (%)	=+12.15 + 2.50*A + 1.17*B-2.50*A*B	0.93	0.91
Moisture (%)	=+31.38–8.83*A-5.50*B + 3.75*A*B	0.96	0.95
WVP (g μm/m^2/d/kPa)	=+302.24–79.67*A-20.00*B + 16.75*A*B-34.34*A2 + 8.66*B2	0.97	0.96

Table 4. Mathematical models and relationships between independent variables and dependent variables.

Thickness, TS and EAB

The thickness of a biofilm or biomarker affects its mechanical properties. Also, the thickness of a film or membrane affects the permeability to water vapor and other gases. Mechanical resistance in films and markers used for smart food packaging is of great importance.

Figure 2 shows contour plot and perturbation curves of the effect of MB and VC on the thickness, TS and EAB of cellulose films. Examining the thickness curves shows that both factors of MB and VC increase the thickness of the film. Considering that cellulosic films have porosity, the placement of MB and VC in these pores as well as the coating of these substances on the surface of cellulosic fibers increases the diameter of cellulosic fibers and ultimately leads to an increase in the thickness of the entire film. According to the results of TS and EAB, both factors, the amount of MB and VC, have reduced the tensile strength and have increased the EAB and flexibility of the film. The effect of MB on reducing the tensile strength and increasing the flexibility of the film has been greater than the effect of VC. Due to the presence of N and S groups in MB and O groups in the structure of VC, the probability of electrostatic interactions and hydrogen bonds between these groups with the OH groups of cellulose is high, which makes these interactions of the cohesion of cellulose polymer chains weaker and reduces its tensile strength and probably increases flexibility for this reason. Shi et al. (2018) modified cellulose film with MB and investigated its structure. The results of their research, from the point of view of the effect of MB on the mechanical properties of cellulose film, confirm the results of the current research to some extent[26]. Also, Atila et al. (2022) have reported the effect of VC on the physical resistance and other characteristics of cellulosic fibers, and their results show relative agreement with the results of the current research[27].

Moisture content and WVP

One of the most important reasons for the spoilage of food products is the presence of moisture inside the package. Based on this, in this work, the moisture content and water vapor permeability of the prepared composite films were investigated. Figure 3 shows contour plot and perturbation curves of the effect of MB and VC on moisture content and WVP of cellulose films. The results of checking the moisture content show that both MB and VC agents have significantly reduced the moisture content. By examining the chemical structure of cellulose, MB and VC, it can be estimated that N and S groups in MB and O groups in VC have electrostatic interactions with the OH groups of cellulose that this phenomenon decreases the hydrogen interactions between the OH groups of cellulose and the H_2O molecule, which leads to a decrease in the amount of water molecules on the cellulose surface and the moisture content decreases.

Also, both factors of MB and VC have reduced the WVP. As discussed earlier, cellulose has a porous structure that is susceptible to the passage of various gases and especially water vapor molecules, which with the composite of this film with MB and VC, these pores are filled to a large extent and the passage of water molecules is blocked and the WVP is reduced. Also, as discussed in the discussion of thickness, MB and VC increase the thickness of cellulose and thus increase the length of the passage of water molecules, which causes a decrease in permeability to water vapor. Tan et al. (2020) have investigated the water resistance and antioxidant properties of chitosan-ascorbate film modified with MB. The results of their research in terms of the effect of MB on the characteristics of water vapor permeability and other characteristics of water resistance are in relative agreement with the results of the current research[28].

Antioxidant and antibacterial property

MB as a phenothiazine dye has the ability to stain biofilm. This dye has antimicrobial effects. MB shows good antibacterial properties by absorbing light. The antibacterial effect of MB is caused by DNA damage, but MB is non-toxic in the human body[29]. Also, MB has oxazine or antioxidant properties. The antioxidant ability of MB is due to the fact that it loses electrons in the presence of oxidizing agents. VC is effective in the survival, destruction and overall metabolism of various bacteria. Although bacteria usually have the ability to ferment VC, this vitamin can expose bacteria to oxidative stress and inhibit bacterial growth[30]. The antioxidant and antimicrobial properties (against *Staphylococcus aureus* and *Escherichia coli*) of Cel/MB/VC have been investigated. Table 5 shows the antioxidant and antibacterial properties of cellulose films containing MB and VC. As it is clear from the results, the pure cellulose film does not have antibacterial properties, but it has a very small amount of antioxidant properties, which is probably related to the physical removal of DPPH radicals by the cellulose film. Both MB and VC have increased antioxidant properties, and the film containing both MB and VC has the highest antioxidant properties. Of course, it is clear that the effect of VC on antioxidant properties is much higher than that of MB. However, VC is a very strong and well-known antioxidant, and the results obtained were expected. Pure cellulose film does not show any antibacterial properties, but films containing MB and VC show good antibacterial properties against both types of bacteria (Gram positive and Gram negative). Cellulose film, which simultaneously contains MB and VC, shows the most antimicrobial properties, which indicates the

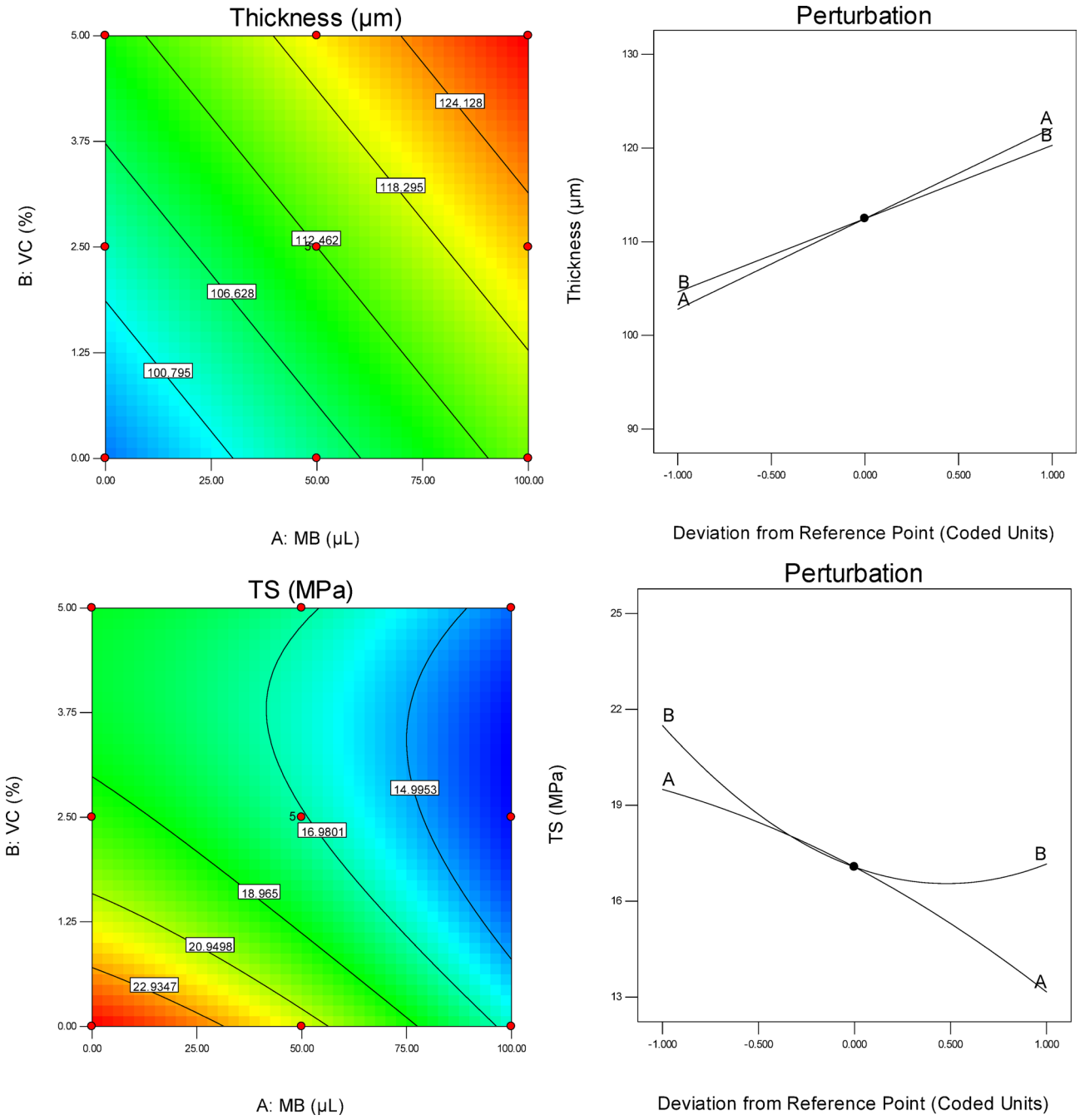

Fig. 2. Contour plot and perturbation curves of the effect of MB and VC on thickness, TS and EAB of cellulose films.

synergy of the antibacterial effect of MB and VC. There are many studies that have reported the antibacterial properties of MB and VC, which confirm the results of the present study[31,32].

SEM images and FTIR spectra

Figure 4 shows SEM images and FTIR spectra of cellulose films and various composites. According to the SEM images, the pure cellulose film has a fibrous structure with dimensions of 20 to 100 nm, which has significant porosity on the surface of the film. By adding MB on the film, the porosity of the film surface has been filled to a large extent and a uniform surface has been created. VC fills most of the surface of the fibers and in the cellulose film containing VC, the surface porosity of the cellulose film is still observed. In the cellulose film containing MB and VC, the surface of the polymer is largely saturated with the additive and the penetration paths of various gases from the surface of the polymer are largely filled. Acharya et al. (2017) have investigated the structure of cellulosic film and modified cellulosic films by SEM technique, and their results are in good agreement with the results of the present research[33].

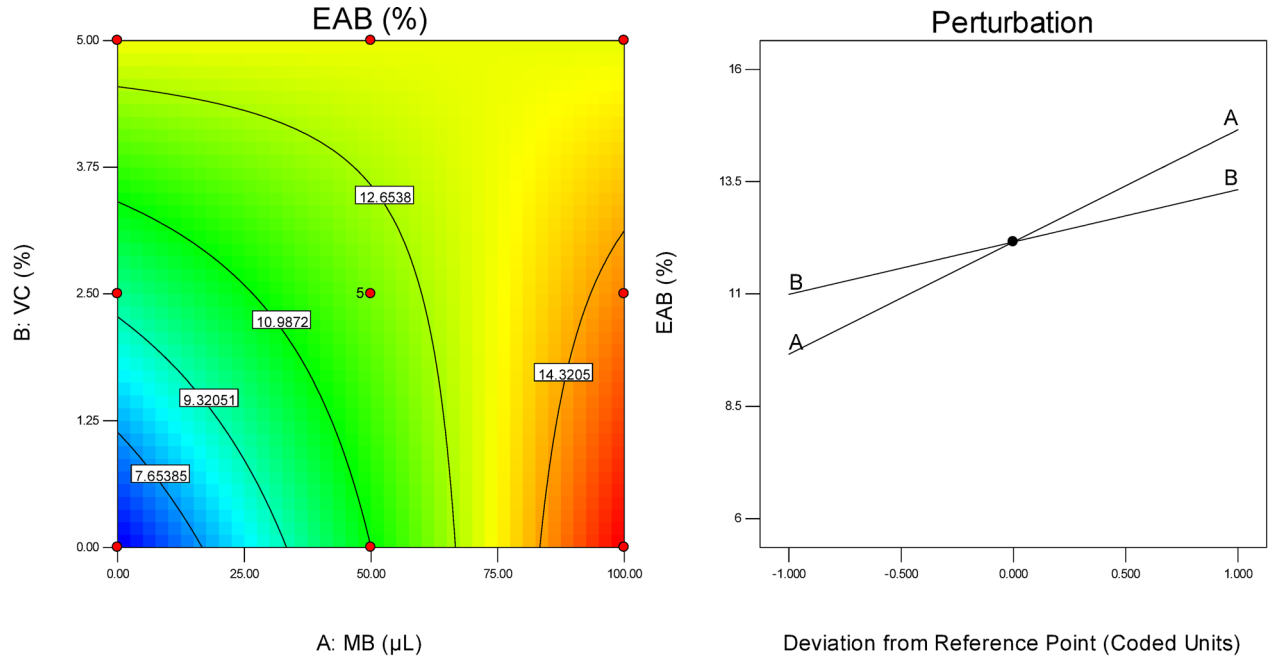

Fig. 2. (continued)

Examination of FTIR spectra confirms the electrostatic interactions between cellulose fibers, MB and VC. In the FTIR spectrum of pure cellulose film, the functional groups of this polymer have been confirmed by different peaks. In this spectrum, peak at 3330 cm^{-1} indicates the stretching vibrations of O-H groups. Peak 2894 represents C-H vibrations in R-CH_2-CH_3 structures. The 1415 peak confirms intra-ring C-C vibrations and the 1152 peak shows C-O stretching vibrations of the C-H bond. Peaks of 1023 and 875 are respectively related to C-O and C-H vibrations connected to different functional groups. By comparing the spectrum of pure cellulose film with its different composites, no significant difference is observed between the spectra because most of the hydrocarbon structure and elements in different composites are similar. But it can be seen that the peaks related to the same functional groups in different composites have appeared in different wave numbers (shifted to higher or lower wave numbers), which indicates the electrostatic interactions between the composite components. Also, in the spectrum of Cel/MB, a new peak has appeared (compared to the pure cellulose film spectrum) at wave number of 1640, which is related to C-N stretching vibrations, which was expected due to the structure of MB. Also, in the spectrum of Cel/VC, two new peaks (compared to the pure cellulose film spectrum) have appeared at wave numbers of 1665 and 1751, which are related to C = C stretching vibrations specific to VC. Hishikawa et al. (2017) investigated the FTIR spectrum of cellulose film[34], Ovchinnikov et al. (2016) investigated the chemical structure of MB using FTIR spectrum[35] and Voss et al. (2018) investigated the FTIR spectrum of polysaccharide film containing VC[36]. The mentioned studies confirm the results of FTIR spectra of the present study.

XRD patterns and TGA curves

Crystalline structure and thermal resistance are characteristics of films that can affect other characteristics of films such as chemical and thermal stability. The type of interaction of additives with cellulose is largely related to the crystalline structure and porosity of cellulose. Figure 5 shows the XRD spectrum and the TGA curve of cellulose films and its various composites.

In the XRD pattern, the pure cellulose film exhibits a semi-crystalline cellulose structure with distinct peaks at 2θ values of 15°, 17°, and 22°, which clearly indicate the crystalline nature of the film and align well with results from previous research.

Furthermore, upon examining the cellulose film modified with methylene blue (MB) and vitamin C (VC), it was found that MB does not significantly impact the crystalline structure of cellulose. In contrast, VC enhances the crystalline properties of the cellulose film. The cellulose film containing VC displays additional peaks at 2θ values of 25°, 27°, 30°, and 33°, all of which correspond to the crystal structure of VC.

The influence of VC on the crystallinity of cellulose may arise from new chemical or electrostatic interactions that affect crystallinity development. The new peaks observed in the VC-containing films confirm the presence of VC in the composite structure. Previous studies, including those by Palma-Rodríguez et al. (2018), Kumar et al. (2018), and Ahmed et al. (2018), validate the presence of these peaks, providing sufficient data to support our discussion[37–39].

The XRD patterns of the present study can be compared to the findings from French AD, Santiago Cintrón (2013)[40] and French AD (2014)[41] as follows: Crystalline Peaks: In this study, the spectra show peaks at 2θ values

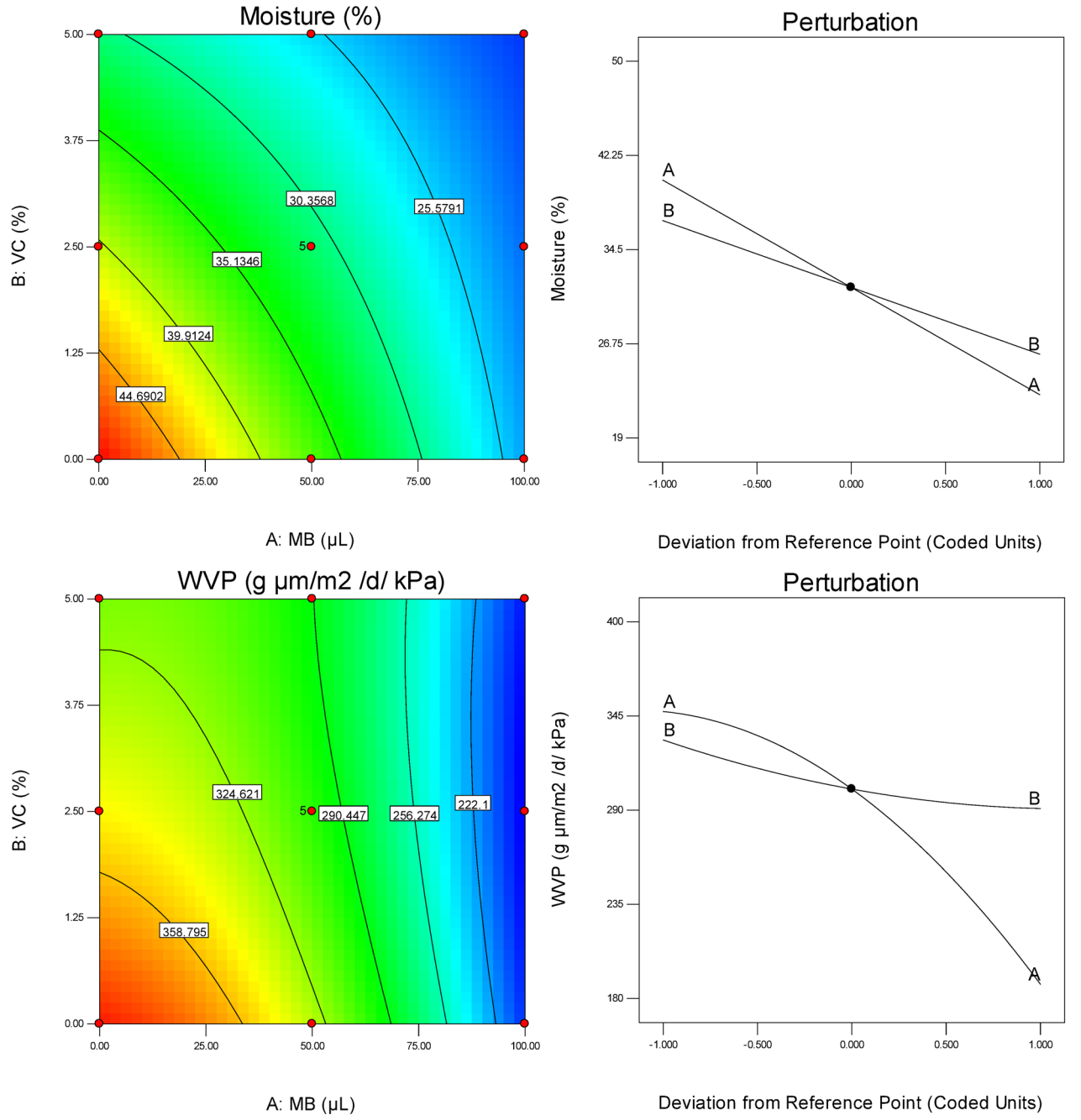

Fig. 3. Contour plot and perturbation curves of the effect of MB and VC on moisture content and WVP of cellulose films.

of 15°, 17°, and 22° for pure cellulose, consistent with the crystalline regions described in French AD (2014), indicating a semi-crystalline structure. Additive Effects: The new peaks at 2θ values of 25°, 27°, 30°, and 33° in the cellulose-VC films may suggest the formation of new crystalline structures rather than an increase in crystallinity, which is consistent with observations in the literature regarding how additives can influence crystallite size and structure. New Peaks Interpretation: These new peaks could indicate changes in the crystalline characteristics of the cellulose due to the presence of vitamin C, aligning with the discussions in French et al. (2014) about interactions that affect crystalline structures in composites.

Film	Antibacterial activity: Inhibition zone diameter (mm)		Antioxidant activity (%)
	Escherichia coli (G-)	*Staphylococcus aureus* (G+)	
Cel	0*	0	4 ± 1^{a}
Cel/MB	6.1 ± 0.4^{b}	10.2 ± 0.3^{b}	42 ± 2^{c}
Cel/VC	10.2 ± 0.2^{c}	12.1 ± 0.4^{c}	64 ± 3^{b}
Cel/MB/VC	12.8 ± 0.3^{c}	14.1 ± 0.5^{c}	82 ± 2^{d}

Table 5. Antioxidant and antibacterial properties of cellulose film and its composites. *Different letters in each column indicate the significance of the difference in means.

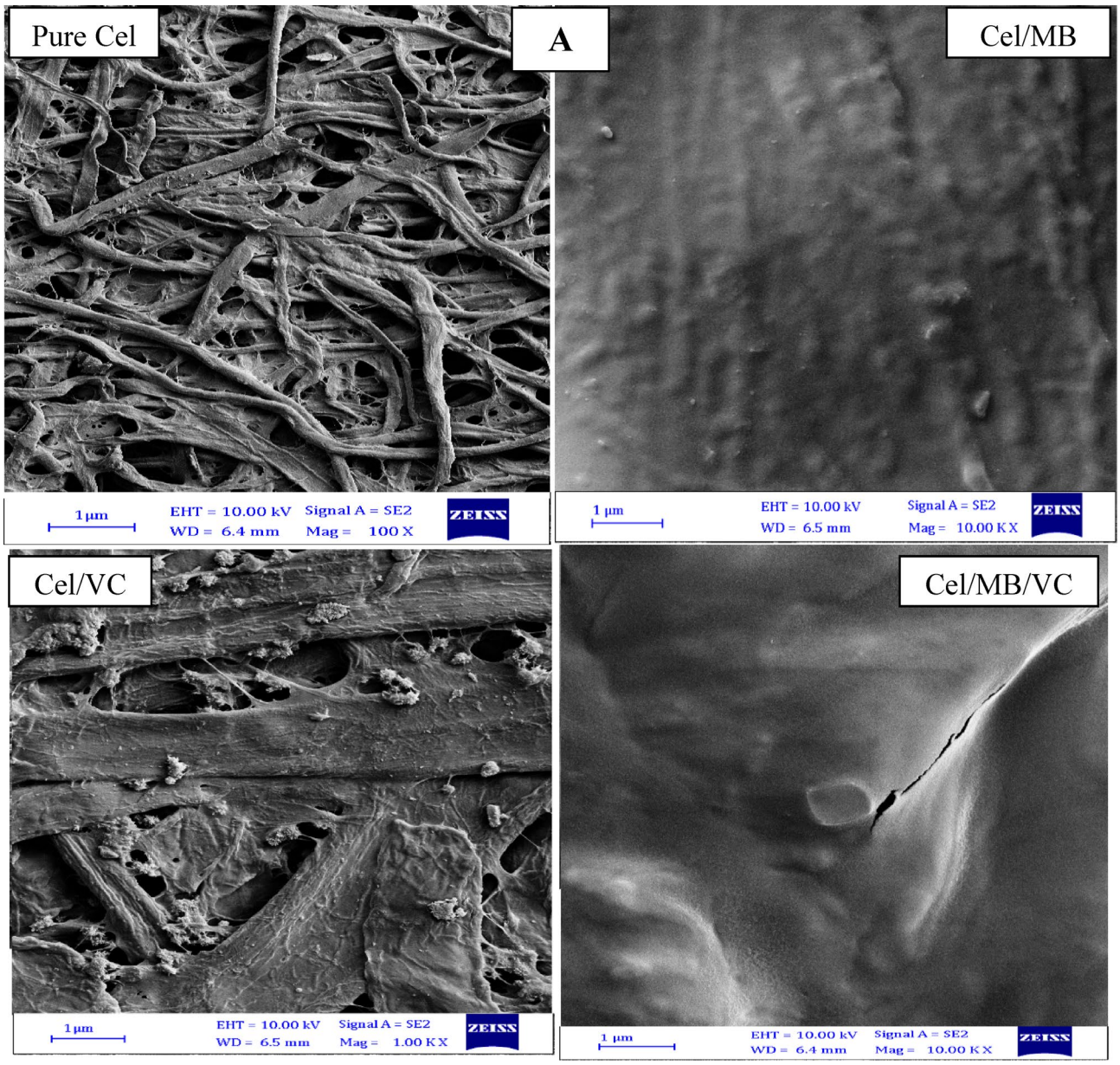

Fig. 4. SEM images (**A**) and FTIR spectra (**B**) of cellulose films and various composites.

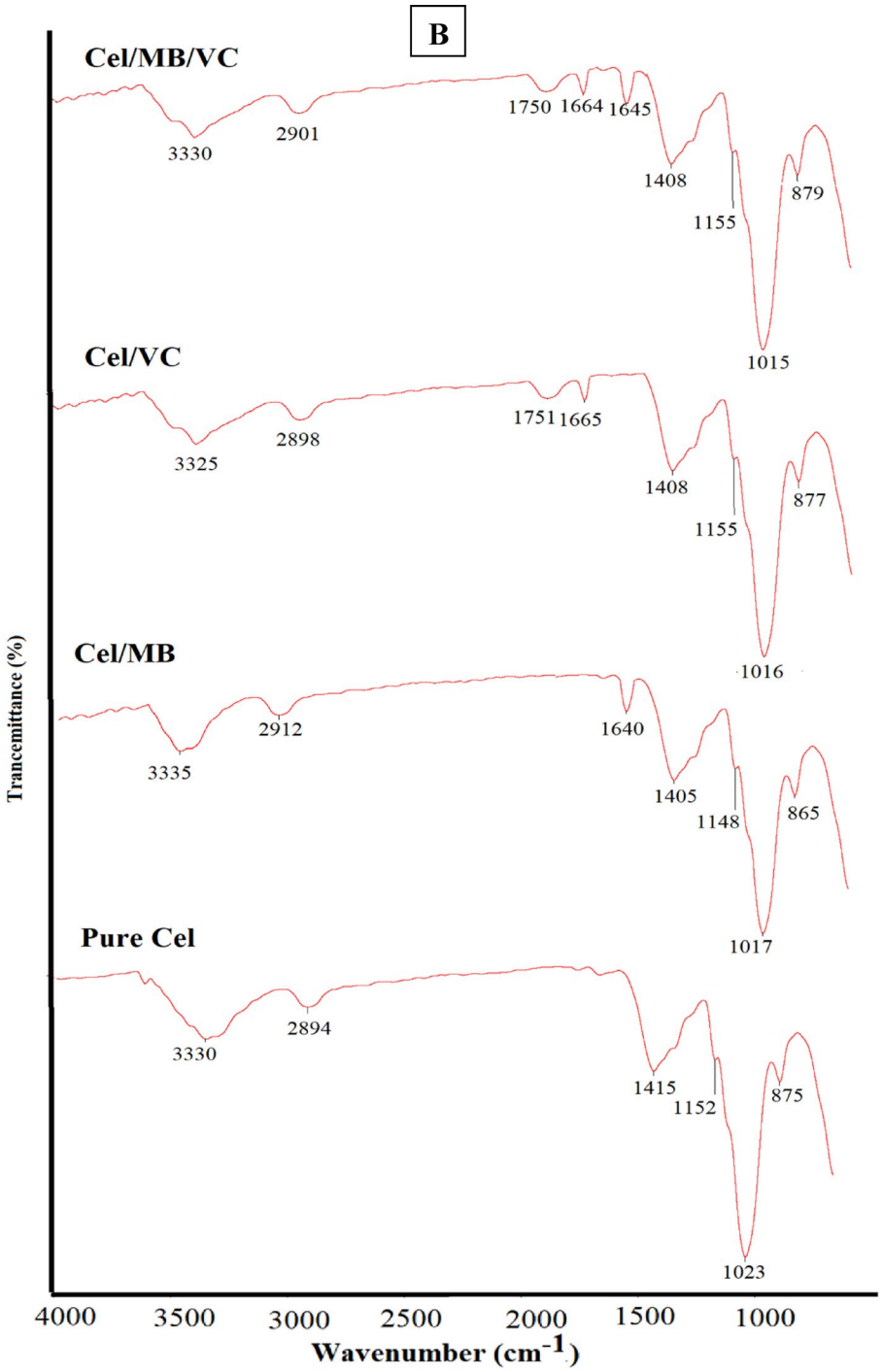

Fig. 4. (continued)

Examining the TGA curves showed that the cellulose film undergoes weight decomposition in two stages. The first stage occurs at a temperature between 70 and 130 °C, which is related to the evaporation of possible water molecules in the film structure. Weight loss at this stage is about 5%. The second stage of decomposition, which is related to the complete destruction of the polymer, takes place at a temperature between 280 and 400 °C. At this stage, 90 to 95% of the polymer is destroyed and destroyed.

By examining the TGA curves of composite films, it was found that by adding MB and VC to the film, the temperature of thermal decomposition increases, and in other words, the thermal resistance of the film is

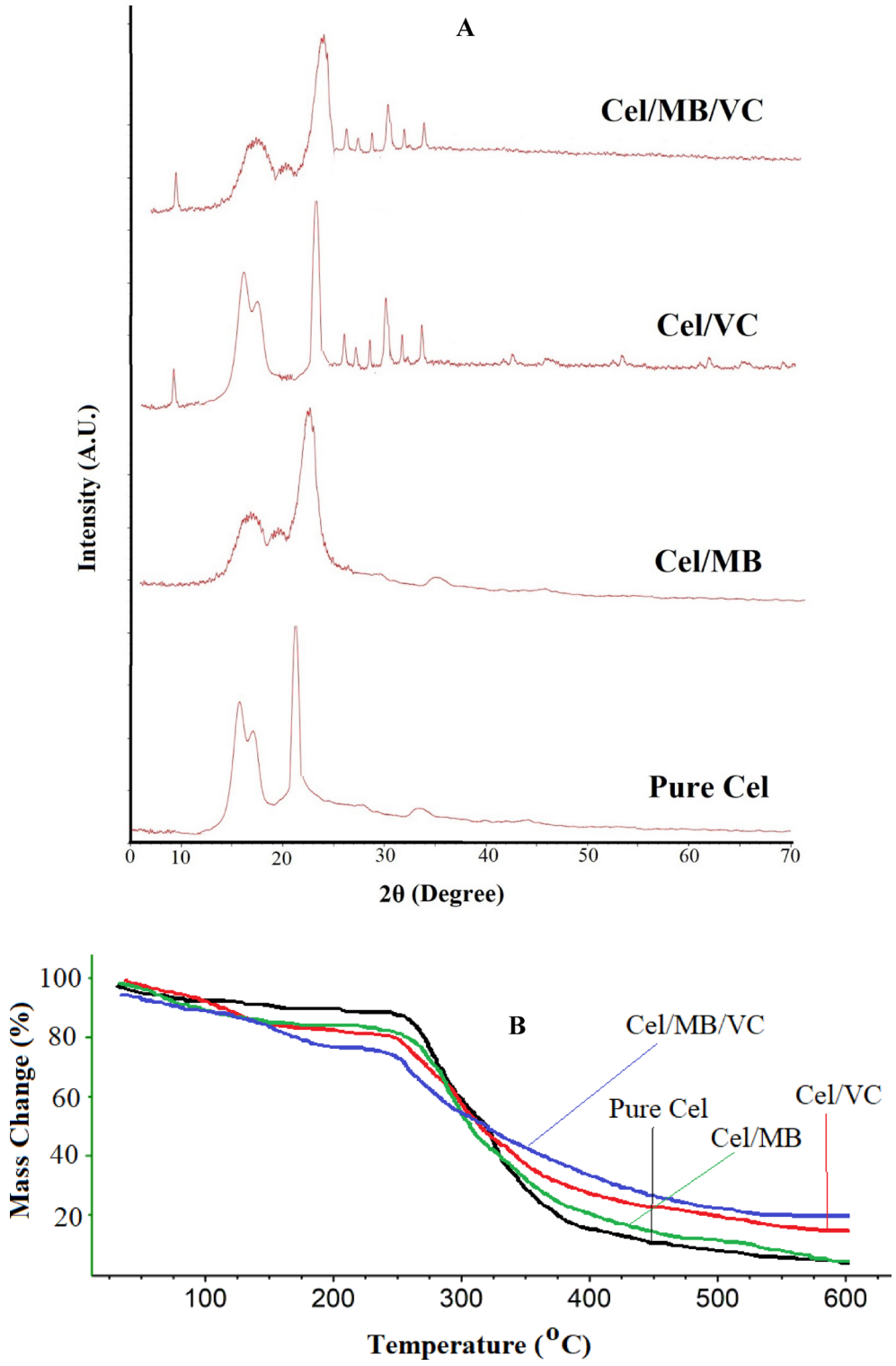

Fig. 5. XRD patterns (**A**) and TGA curves (**B**) of cellulose films and its various composites.

improved. MB can improve the thermal resistance of films by preventing chemical degradation and oxidation at high temperatures. VC can prevent oxidation in the raw materials and therefore increase their thermal stability. The cellulose film containing both MB and VC has the highest decomposition temperature and the highest thermal resistance, which indicates the synergistic effect of these two substances. It can be said that the electrostatic interactions between the composite components, which were also mentioned in the analysis of the FTIR spectra, have led to the improvement of the thermal resistance of the cellulose film. Nurazzi et al. (2022)

have investigated the thermal resistance and crystal structure of cellulose films and its composites, and their results are in good agreement with the results of the present research[42].

Absorption rate and release of MB

Figure 6 shows the one-factor curve of MB absorption rate on cellulose film and the three-dimensional curve of the effect of the initial amount of MB and VC concentration on the rate of release of MB from cellulose films containing this substance. As it is known, the higher the amount of MB used to prepare the composite film, the higher the amount of absorption on the film, which seems to be a natural result, because the higher the amount of MB, the higher the amount of particles available to the cellulosic fibers. Also, the more MB absorbed on the cellulose film, the higher its release rate will be. An important result that can be seen is that in the composite films where VC is present along with MB in the film, the amount of MB release has decreased a lot. This result is due to the oxidation-reduction interaction of MB and VC, as well as VC, which is added during the production stage after the stabilization of MB on cellulose, acts like a coating and prevents its release. The point that should be noted is that the maximum release of MB from films containing MB and VC was around 15%, which according to some sources reported that MB was not recommended for oral consumption, it seems that this amount of release is problematic, but it should be noted that the Cel/MB/VC film is designed for the intelligent packaging of oily products to delay the oxidation of oils and also show its expiration time, but In this research, the rate of release in water is reported, and it is likely that the rate of release of MB in oils will be much lower. In a similar research, Khakpour et al. (2023) have used starch film containing lycopene pigment as a nitrite detection kit, and the results of their research in terms of the application and performance of the sensor in identifying oxidants in food products show relative agreement with the results of the current research[43].

Application of film as H_2O_2 sensor (kit)

4 films according to Table 3 were used to check the performance of films to identify oxidizing agents (H_2O_2). To use the films as a kit, these films were cut in dimensions of 1 × 4 cm. In these films, due to the fact that VC is a reducing substance and due to the fact that MB is colorless in its reduced form, the color of these films is white (the main color of cellulose as the base of the kit). Adding oxidizing agents such as hydrogen peroxide to the surface of the kit changes the color of the kit from white to blue. The amount and intensity of color changes of the sensor depend on the concentration of the oxidizing agent. Therefore, a mathematical relationship is established between the concentration of the oxidizing agent and the color changes, through which the prepared kits can be calibrated with respect to the oxidizing agents, and the prepared calibration curve can be used to obtain the amount and concentration of the oxidizing agent. In this study, hydrogen peroxide was used as a soft oxidizer to investigate the behavior of the prepared sensors. Figure 1-B shows the color changes of the sensor in different concentrations of hydrogen peroxide. Table 6 shows the figure of merits of the 4 prepared kits compared to hydrogen peroxide.

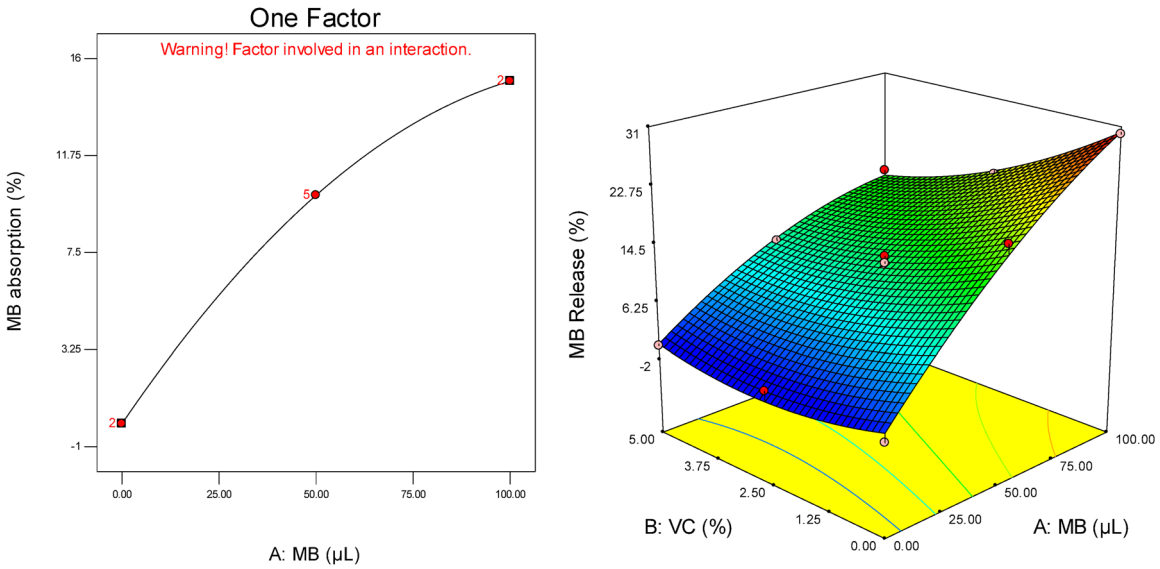

Fig. 6. One-factor curve of the effect of MB on the MB absorption rate and three-dimensional curve of the effect of the initial amount of MB and VC on the rate of MB release.

Kit	DL (mg/100 ml)	LR (mg/100 ml)	S (100 ml/mg)	R^2
K1 (Cel/MB50/VC2.5)	6.12	6.12–22	0.1549	0.997
K2 (Cel/MB50/VC5)	8.4	8.4–25	0.1742	0.998
K3 (Cel/MB100/VC2.5)	2	2–21	0.2526	0.998
K4 (Cel/MB100/VC5)	1.9	2.1–20	0.2995	0.999

Table 6. Figure of merits of the H_2O_2 kits based on the b (color factor) compared to the H_2O_2 concentration. DL: Detection limit, LR: Liner range, S: Sensitivity, R^2: Coefficient of determination.

As it is clear from the results of this table, the cellulose film containing the highest amount of MB and the highest amount of VC shows the highest sensitivity to hydrogen peroxide oxidant. It is known that by increasing the amount of MB on the surface of the film, the amount of this active substance that is available to the oxidant also increases, and causes even small amounts of the oxidant to cause significant color changes on the surface of the film, which causes The detection limit of the sensor to measure the oxidant should also be reduced. It should be mentioned that in the examination of sensors, the lower the detection limit of the sensor is, it indicates the high detection power of the sensor and the high sensitivity of the sensor. Jiang et al. (2013) have used silica/cellulose composite modified with catalytic enzymes as a sensor to measure hydrogen peroxide. Considering the use of enzyme and catalytic structure in the mentioned study, it should be noted that the present research has presented a simpler, cheaper and more accessible system compared to the research of Jiang et al. Also, Jiang et al.'s results show a good match with the results of the current research in terms of the application of the sensor and the functional system of the sensor[44].

Conclusion

In this study, a novel active and intelligent biodegradable film was developed. The film was created by modifying cellulose nanofibers with MBVC. Hydrogen peroxide was employed as a mild oxidizing agent to assess the sensing capabilities of the modified cellulose film. Analysis of the film's thickness indicated that the incorporation of MB and VC resulted in an increase in thickness. Furthermore, the presence of these agents led to a reduction in TS while enhancing the EAB. Notably, MB and VC significantly lowered the moisture content of the film, as well as the WVP. While the pure cellulose film exhibited minimal antioxidant properties and lacked antibacterial activity, the addition of MB and VC markedly enhanced its antioxidant capabilities. The films containing MB and VC demonstrated substantial activity against both Gram-positive and Gram-negative bacteria. The pure cellulose film maintained a fibrous structure with dimensions ranging from 20 to 100 nm. MB largely filled the porosity of the film's surface. FTIR spectroscopy confirmed the presence of electrostatic interactions among the cellulose fibers, MB, and VC. While MB did not significantly alter the crystalline structure of cellulose, VC enhanced its crystalline characteristics. The electrostatic interactions among the composite components contributed to improved thermal stability of the cellulose film. The maximum release rate of MB from the films was approximately 15%. Notably, the cellulose film with the highest concentrations of both MB and VC exhibited the greatest sensitivity to hydrogen peroxide.

Data availability

The data that support the findings of this study are available from the corresponding author upon reasonable request.

Received: 16 October 2024; Accepted: 16 June 2025
Published online: 02 July 2025

References

1. Pal, D. & Sen, S. Emerging petroleum pollutants and their adverse effects on the environment. In *Impact of Petroleum Waste on Environmental Pollution and its Sustainable Management Through Circular Economy* 103–137 (Springer Nature Switzerland, 2024).
2. Yin, Y. & Woo, M. W. Transitioning of petroleum-based plastic food packaging to sustainable bio-based alternatives. *Sustainable Food Technol.* **2** (3), 548–566 (2024).
3. Pirsa, S. & Mohammadi, B. Conducting/biodegradable chitosan-polyaniline film; antioxidant, color, solubility and water vapor permeability properties. *Main Group Chem.* **20** (2), 133–147 (2021).
4. Colnik, M., Knez-Hrnčič, M., Škerget, M. & Knez, Ž. Biodegradable polymers, current trends of research and their applications, a review. *Chem. Ind. Chem. Eng. Q.* **26** (4), 401–418 (2020).
5. Pirsa, S., Mahmudi, M. & Ehsani, A. Biodegradable film based on Cress seed mucilage, modified with lutein, maltodextrin and alumina nanoparticles: physicochemical properties and lutein controlled release. *Int. J. Biol. Macromol.* **224**, 1588–1599 (2023).
6. Tanpichai, S., Srimarut, Y., Woraprayote, W. & Malila, Y. Chitosan coating for the Preparation of multilayer coated paper for food-contact packaging: wettability, mechanical properties, and overall migration. *Int. J. Biol. Macromol.* **213**, 534–545 (2022).
7. Tanpichai, S. et al. Mechanical and antibacterial properties of the Chitosan coated cellulose paper for packaging applications: effects of molecular weight types and concentrations of Chitosan. *Int. J. Biol. Macromol.* **155**, 1510–1519 (2020).
8. Liu, Y. et al. *A Review of Cellulose and its Derivatives in biopolymer-based for Food Packaging Application*112pp.532–546 (Trends in Food Science & Technology, 2021).
9. Yorghanlu, R. A., Hemmati, H., Pirsa, S. & Makhani, A. Production of biodegradable sodium caseinate film containing titanium oxide nanoparticles and grape seed essence and investigation of physicochemical properties. *Polym. Bull.* **79** (10), 8217–8240 (2022).
10. Farooq, A. et al. Cellulose from sources to nanocellulose and an overview of synthesis and properties of nanocellulose/zinc oxide nanocomposite materials. *Int. J. Biol. Macromol.* **154**, 1050–1073 (2020).

11. Erfani, A., Pirouzifard, M. K. & Pirsa, S. Photochromic biodegradable film based on polyvinyl alcohol modified with silver chloride nanoparticles and spirulina; investigation of physicochemical, antimicrobial and optical properties. Food Chemistry, 411, p.135459. (2023).
12. Gupta, P. K. et al. An update on overview of cellulose, its structure and applications. Cellulose, 201(9), p.84727. (2019).
13. Reis, D. T., dos Santos Pereira, A. K., Scheidt, G. N. & Pereira, D. H. *Plant and Bacterial Cellulose: Production, Chemical Structure, Derivatives and Applications*pp.321–329 (The Electronic Journal of Chemistry, 2019).
14. Mills, A., Hazafy, D., Parkinson, J., Tuttle, T. & Hutchings, M. G. Effect of alkali on methylene blue (CI basic blue 9) and other thiazine dyes. *Dyes Pigm.* **88** (2), 149–155 (2011).
15. Cwalinski, T. et al. Methylene blue—current knowledge, fluorescent properties, and its future use. Journal of clinical medicine, 9(11), p.3538. (2020).
16. Fweja, L. W. T., Lewis, M. J. & Grandison, A. S. The Potential of Conductivity, Redox Potential and Dissolved Oxygen in Raw Milk Quality Prediction. Huria: Journal of the Open University of Tanzania, 15(1), pp.52–70. (2013).
17. Rajeswari, P. V., Sharma, S. K., Ram, S. & Pradhan, D. Nanoporous N/O: sp2-C films functionalized at nonbonding electrons of a biogenic husk (green chili) with deep UV-visible light absorption-emission for photocatalysis and other applications. *Surf. Interfaces*. **38**, 102824 (2023).
18. Pehlivan, F. E. Vitamin C: an antioxidant agent. *Vitam. C.* **2**, 23–35 (2017).
19. Chiarappa, G. et al. Mathematical modeling of L-(+)-ascorbic acid delivery from pectin films (packaging) to agar hydrogels (food). *J. Food Eng.* **234**, 73–81 (2018).
20. Abdolsattari, P., Peighambardoust, S. J., Pirsa, S., Fasihnia, S. H. & Peighambardoust, S. H. Investigating microbial properties of traditional Iranian white cheese packed in active LDPE films incorporating metallic and organoclay nanoparticles. *Chem. Rev. Lett.* **3** (4), 168–174 (2020).
21. Shabkhiz, M. A., Pirouzifard, M. K., Pirsa, S. & Mahdavinia, G. R. Alginate hydrogel beads containing Thymus daenensis essential oils/Glycyrrhizic acid loaded in β-cyclodextrin. Investigation of structural, antioxidant/antimicrobial properties and release assessment. Journal of Molecular Liquids, 344, p.117738. (2021).
22. Abdolsattari, P., Rezazadeh-Bari, M. & Pirsa, S. Smart film based on polylactic acid, modified with polyaniline/zno/cuo: investigation of physicochemical properties and its use of intelligent packaging of orange juice. *Food Bioprocess Technol.* **15** (12), 2803–2825 (2022).
23. Mustafa, F. & Andreescu, S. Chemical and biological sensors for food-quality monitoring and smart packaging. Foods, 7(10), p.168. (2018).
24. Khwaldia, K. Physical and mechanical properties of hydroxypropyl methylcellulose–coated paper as affected by coating weight and coating composition. *BioResources* **8** (3), 3438–3452 (2013).
25. Alizadeh, S., Pirsa, S. & Amiri, S. Development of a colorimetric sensor based on nanofiber cellulose film modified with ninhydrin to measure the formalin index of fruit juice. International Journal of Biological Macromolecules, 253, p.127035. (2023).
26. Shi, C., Tao, F. & Cui, Y. Evaluation of nitriloacetic acid modified cellulose film on adsorption of methylene blue. *Int. J. Biol. Macromol.* **114**, 400–407 (2018).
27. Atila, D., Karataş, A., Keskin, D. & Tezcaner, A. Pullulan hydrogel-immobilized bacterial cellulose membranes with dual-release of vitamin C and E for wound dressing applications. *Int. J. Biol. Macromol.* **218**, 760–774 (2022).
28. Tan, W. et al. Preparation and physicochemical properties of antioxidant Chitosan ascorbate/methylcellulose composite films. *Int. J. Biol. Macromol.* **146**, 53–61 (2020).
29. Calanna, F. et al. Debridement, antibiotic pearls, and retention of the implant (DAPRI): a modified technique for implant retention in total knee arthroplasty PJI treatment. Journal of Orthopaedic Surgery, 27(3), p.2309499019874413. (2019).
30. Majtan, J., Sojka, M., Palenikova, H., Bucekova, M. & Majtan, V. Vitamin C enhances the antibacterial activity of honey against planktonic and biofilm-embedded bacteria. Molecules, 25(4), p.992. (2020).
31. Thesnaar, L., Bezuidenhout, J. J., Petzer, A., Petzer, J. P. & Cloete, T. T. Methylene blue analogues: In vitro antimicrobial minimum inhibitory concentrations and in silico pharmacophore modelling. European Journal of Pharmaceutical Sciences, 157, p.105603. (2021).
32. Mumtaz, S. et al. Evaluation of antibacterial activity of vitamin C against human bacterial pathogens. *Brazilian J. Biology*. **83**, e247165 (2021).
33. Acharya, S., Hu, Y., Moussa, H. & Abidi, N. Preparation and characterization of transparent cellulose films using an improved cellulose dissolution process. *J. Appl. Polym. Sci.*, **134**(21). (2017).
34. Hishikawa, Y., Togawa, E. & Kondo, T. Characterization of individual hydrogen bonds in crystalline regenerated cellulose using resolved polarized FTIR spectra. *ACS Omega*. **2** (4), 1469–1476 (2017).
35. Ovchinnikov, O. V. et al. *Manifestation of Intermolecular Interactions in FTIR Spectra of Methylene Blue Molecules*86pp.181–189 (Vibrational Spectroscopy, 2016).
36. Voss, G. T. et al. Polysaccharide-based film loaded with vitamin C and propolis: A promising device to accelerate diabetic wound healing. *Int. J. Pharm.* **552** (1–2), 340–351 (2018).
37. Palma-Rodríguez, H. M., Alvarez-Ramírez, J. & Vargas-Torres, A. Using modified starch/maltodextrin microparticles for enhancing the shelf life of ascorbic acid by the spray-drying method. *Starch-Stärke* **70** (7–8), 1700323 (2018).
38. Kumar, T. S. M. et al. All-cellulose composite films with cellulose matrix and Napier grass cellulose fibril fillers. *Int. J. Biol. Macromol.* **112**, 1310–1315 (2018).
39. Ahmed, I. et al. Vitamin c/stearic acid hybrid monolayer adsorption at air–water and air–solid interfaces. *ACS Omega*. **3** (11), 15789–15798 (2018).
40. French, A. D. & Santiago Cintrón, M. *Cellulose Polymorphy, Crystallite Size, and the Segal Crystallinity Index*20pp.583–588 (Cellulose, 2013).
41. French, A. D. Idealized powder diffraction patterns for cellulose polymorphs. *Cellulose* **21** (2), 885–896 (2014).
42. Nurazzi, N. M. et al. Thermogravimetric analysis (TGA) and differential scanning calorimetry (DSC) of pla/cellulose composites. In Polylactic acid-based Nanocellulose and Cellulose Composites (145–164). CRC. (2022).
43. Khakpour, F., Pirsa, S. & Amiri, S. Modified starch/cro/lycopene/gum Arabic nanocomposite film: preparation, investigation of physicochemical properties and ability to use as nitrite kit. *J. Polym. Environ.* **31** (9), 3875–3893 (2023).
44. Jiang, Y. et al. Enzyme-mimetic catalyst-modified nanoporous SiO2–cellulose hybrid composites with high specific surface area for rapid H2O2 detection. *ACS Appl. Mater. Interfaces*. **5** (6), 1913–1916 (2013).

Author contributions

Sajad Pirsa conceived of the presented idea, Narmela Asefi developed the theory and performed the computations. Sajad Pirsa verified the analytical methods. Sina Sadeghi discussed the results and contributed to the final manuscript. Sina Sadeghi out the experiment. Sajad Pirsa and Mehdi Gharekhani wrote the manuscript and revised it.

Funding

The author(s) received no financial support for the research, authorship, and/or publication of this article.

Declarations

Competing interests
The authors declare no competing interests.

Conflict of interest
There is not any Conflict of interest between authors.

Ethical approval
Ethical approval for the study was obtained from the relevant local ethics committees.

Consent to participate
All authors consent to participate in the research project.

Consent to publish
All authors consent to publish the current manuscript.

Additional information
Correspondence and requests for materials should be addressed to S.P.

Reprints and permissions information is available at www.nature.com/reprints.

Publisher's note Springer Nature remains neutral with regard to jurisdictional claims in published maps and institutional affiliations.